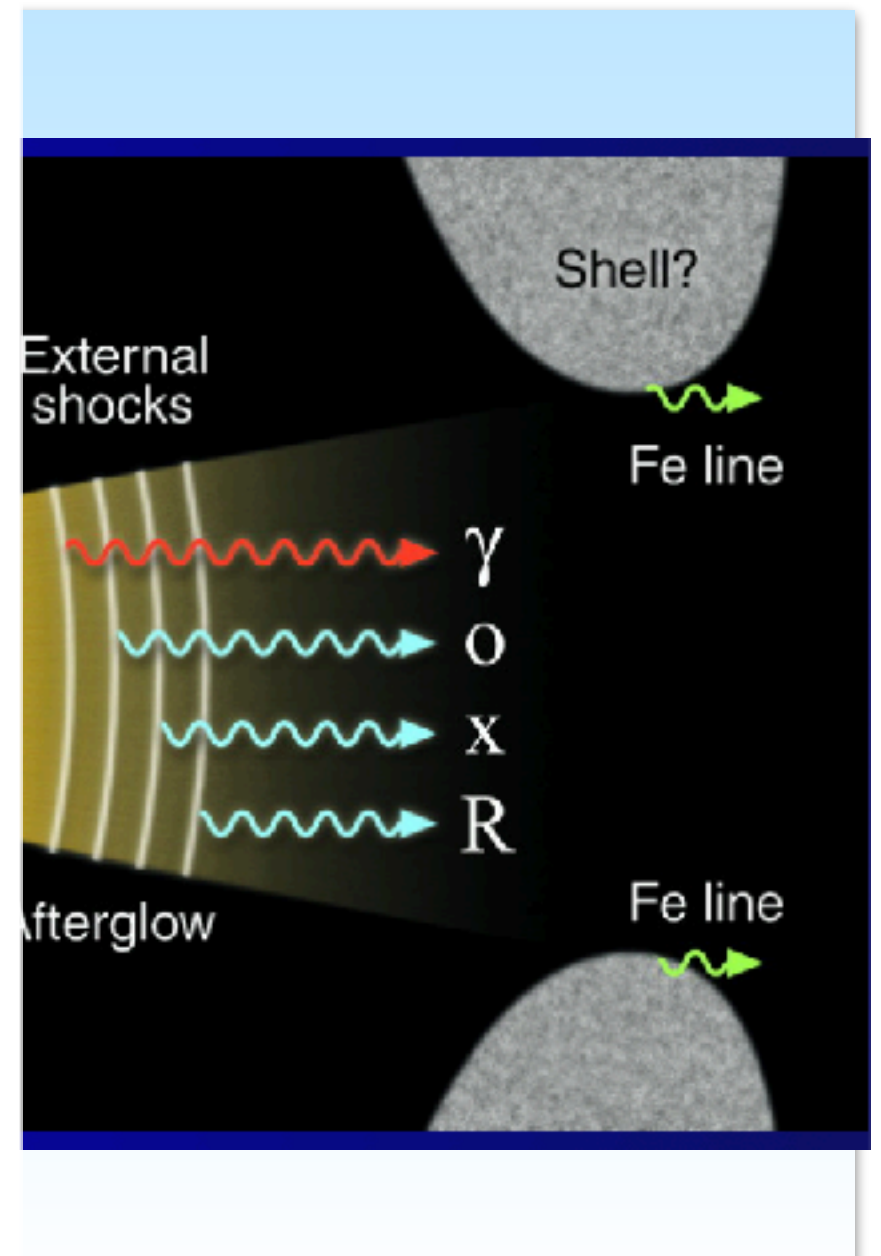
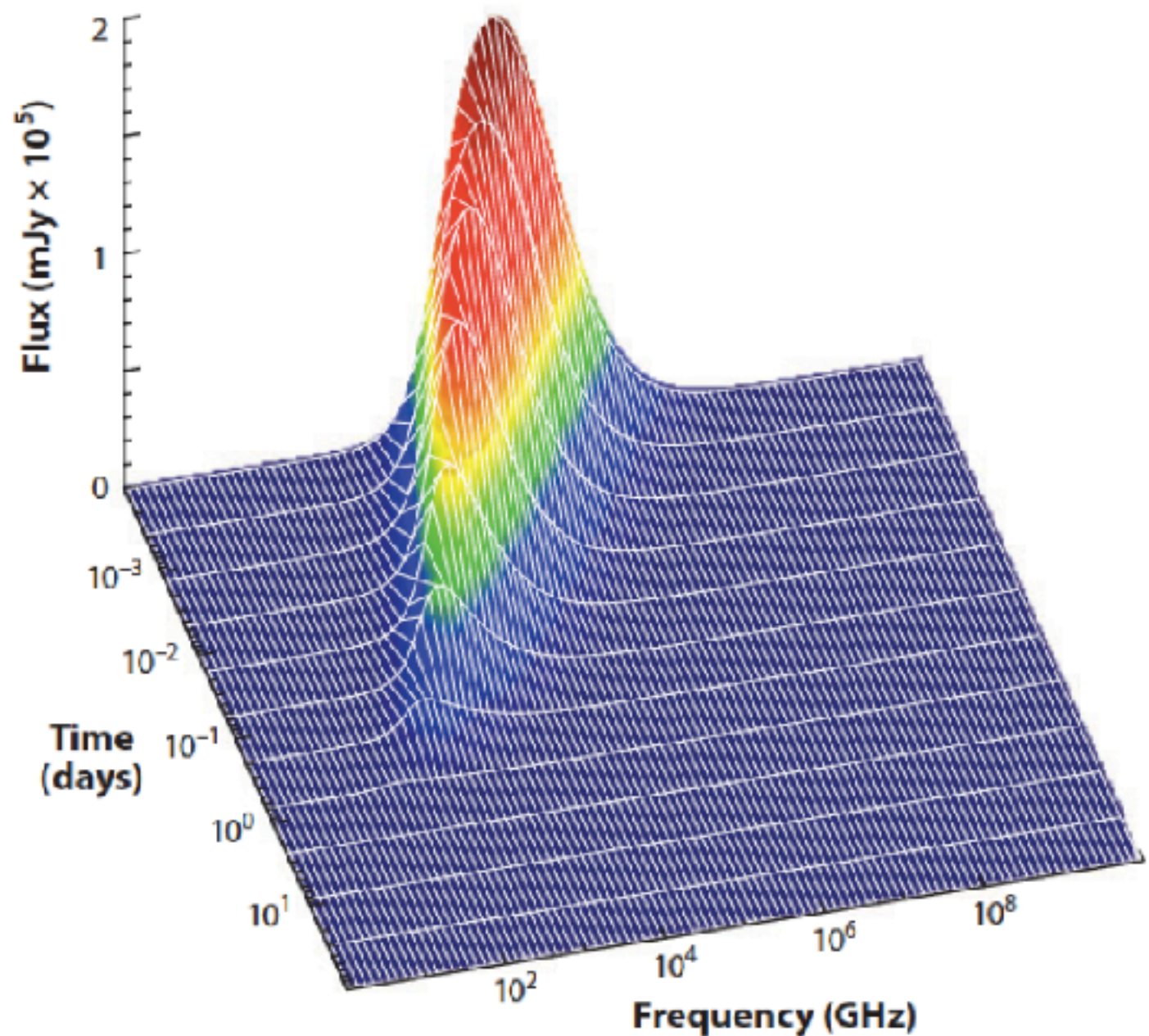


Radio afterglows of GRBs

Poonam Chandra
National Centre for Radio Astrophysics
Tata Institute of Fundamental Research



Radio afterglows



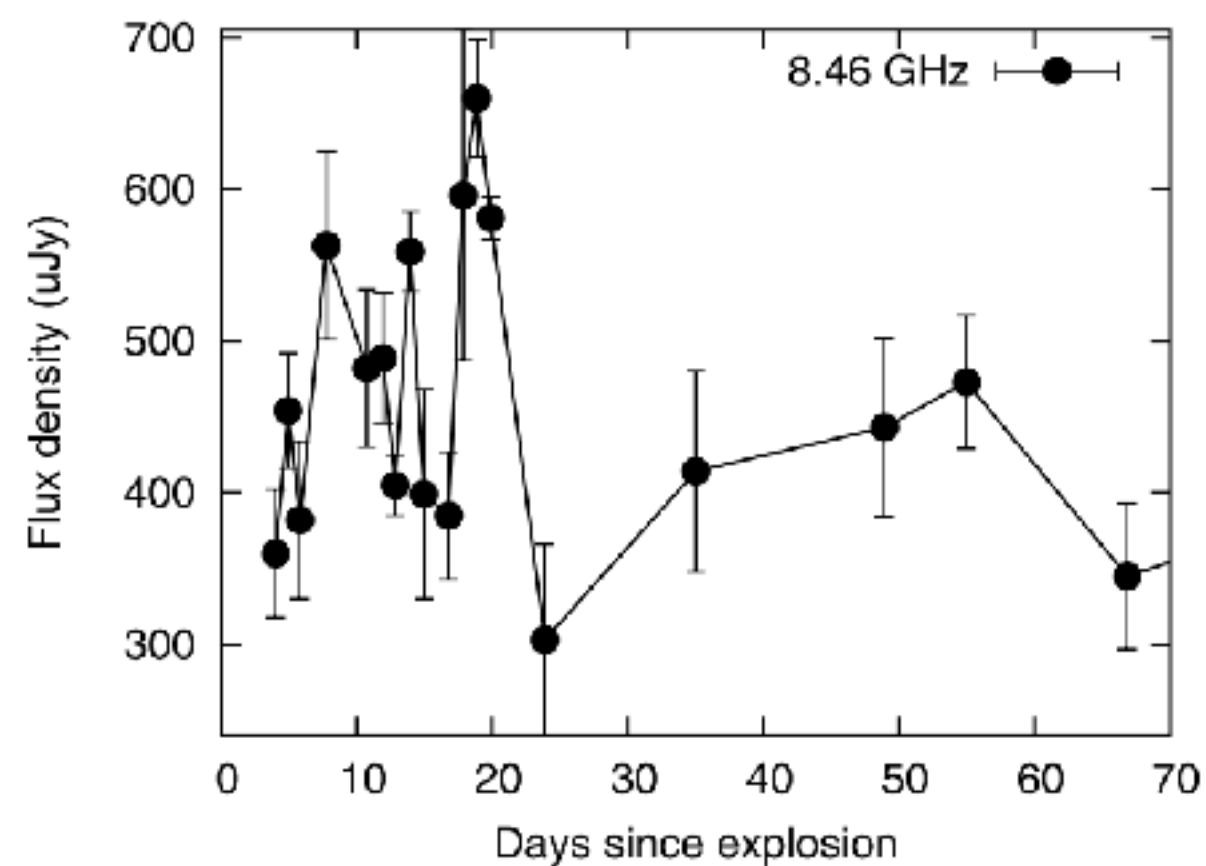
Radio afterglows

- GRB 970508- First GRB discovered in the radio bands.
- Radio afterglow - long lived (several days to months)
- Radio observations present the possibility of following the full evolution of the fireball emission through all of its different stages; first, interstellar scintillation (size constraints (Frail et al. 1997, PC et al. 2008)) synchrotron self absorbed light curve while it is optically thick (density constraints, (Harrison et al. 2001; Panaiteescu & Kumar 2001; Yost et al. 2003; Chandra et al. 2008; Cenko et al. 2011).), then as it slowly rises to a peak flux density and thereafter decays, making a transition from an ultrarelativistic to subrelativistic shock (energetics (Frail et al. 2000, Frail et al. 2005, van Der Horst 2008)).
- Detected at high redshifts (Frail et al. 2006; Chandra et al. 2010) due to the negative k -correction effect (Ciardi & Loeb 2000).

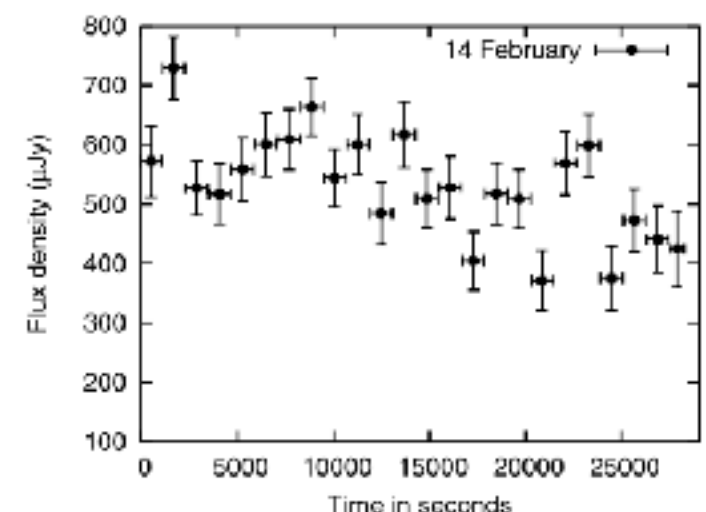
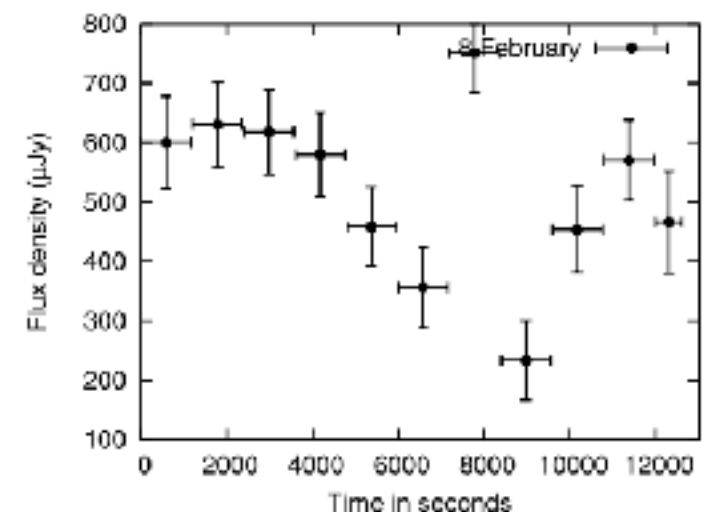
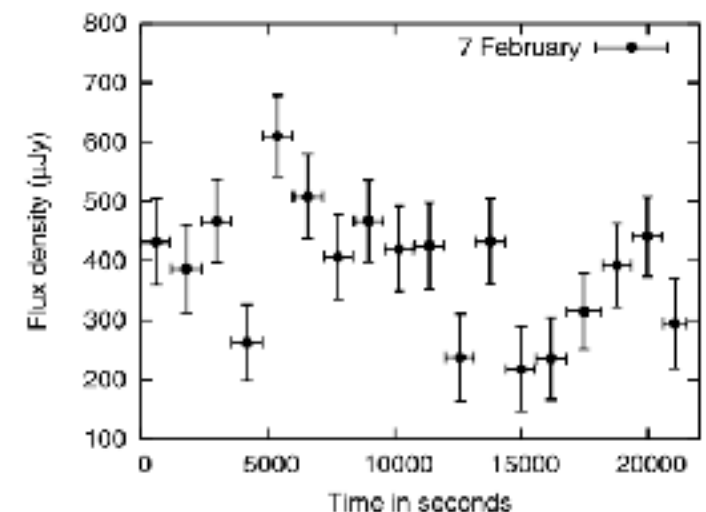
Early radio observations

- Scintillation: inhomogeneities in the local interstellar medium manifest themselves in the form of interstellar scintillations and cause modulations in the radio flux density of a point source whose angular size is less than the characteristic angular size for scintillations .
- GRB 970508: The initial radio flux density fluctuations were interpreted as interstellar scintillations, which lead to an estimation of the fireball size ([Frail et al. 1997a,b](#); [Waxman, Kulkarni & Frail 1998](#)). They deduced the size of the burst to be about 3 microarcseconds.
- GRB 070125: Diffractive scintillation - strong size constraints

Scintillations in GRB 070125



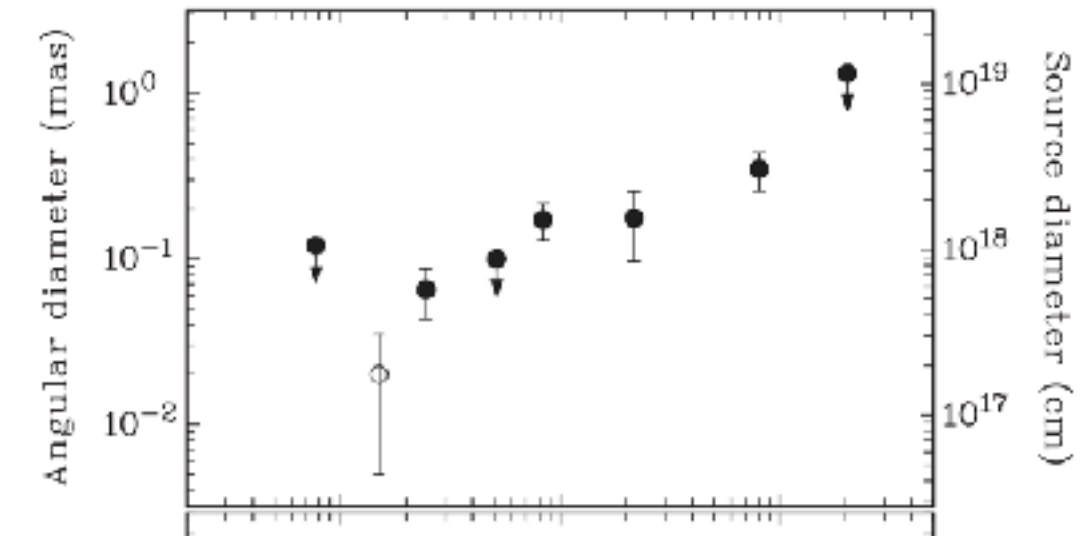
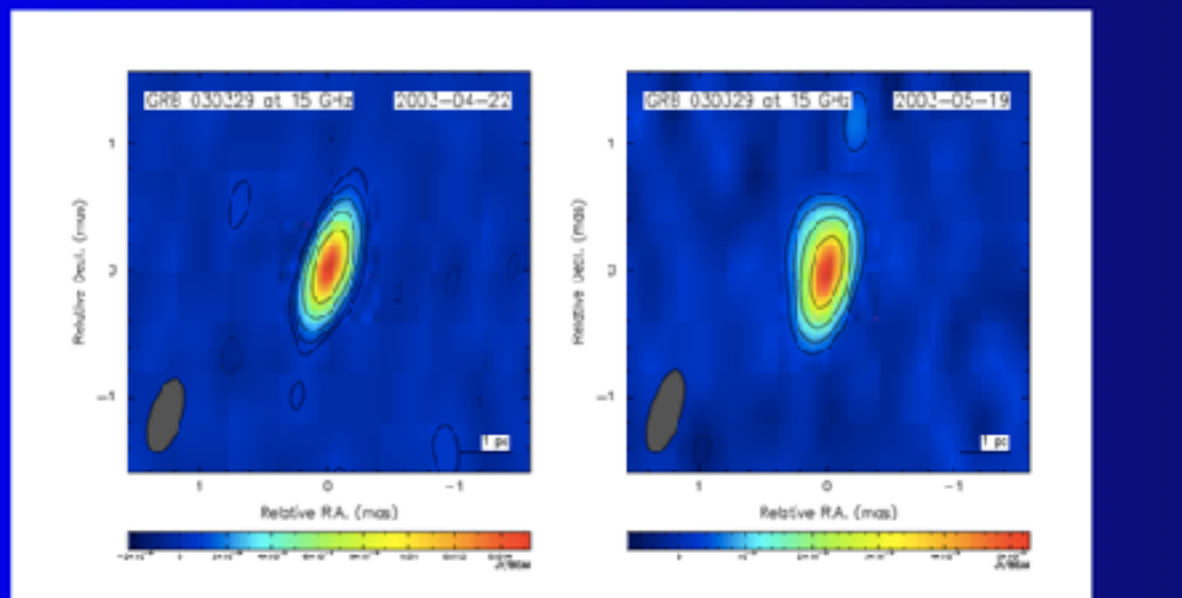
PC et al. 2008



Rare and robust - VLBI

GRB 030329 VLBI: Size 0.07mas
(0.2pc) 25 days and 0.17mas
(0.5pc) 83 days.

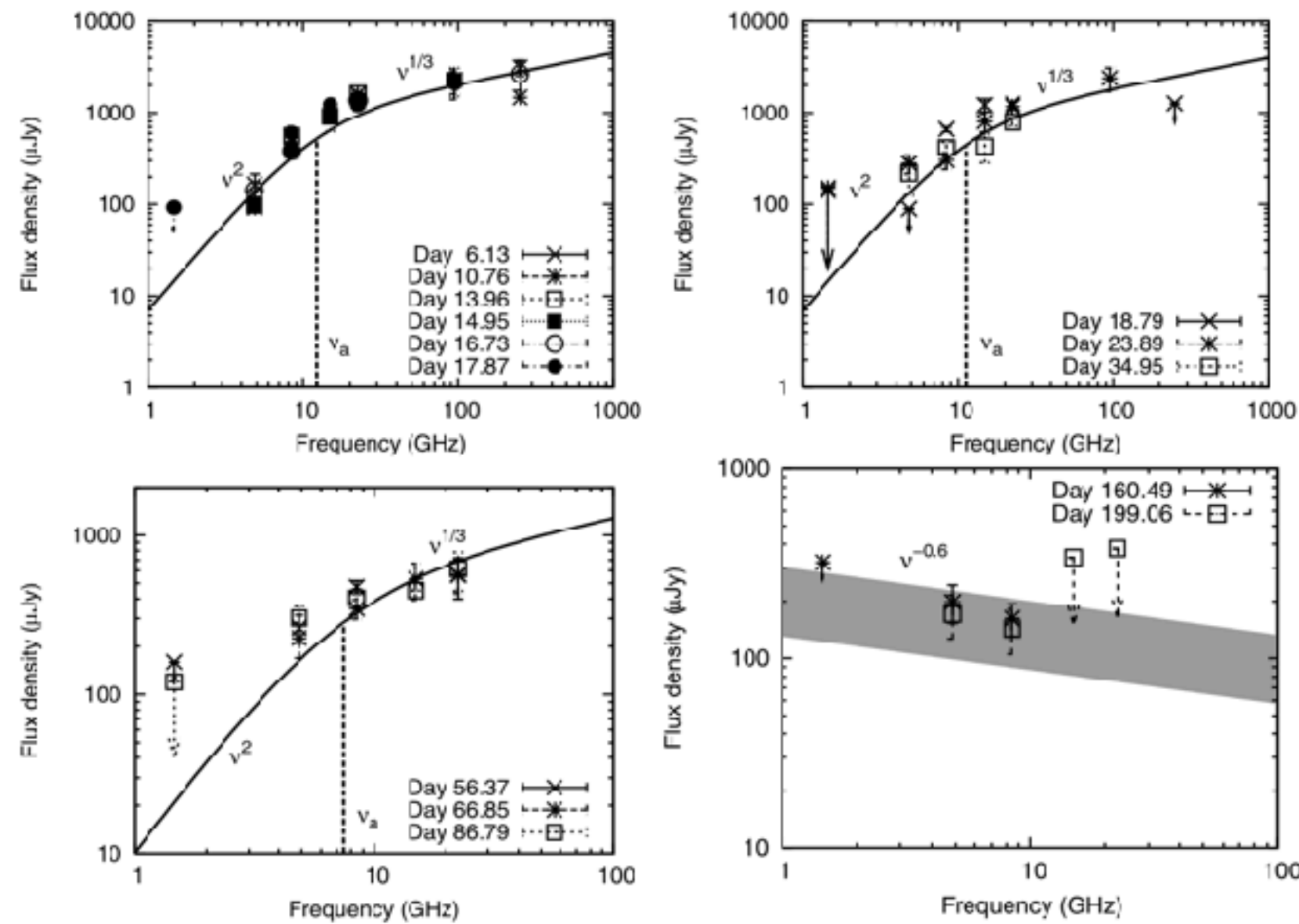
Taylor et al. 2004



Taylor 2004, 2005,
Philstrom et al. 2007,
Mesler et al. 2012

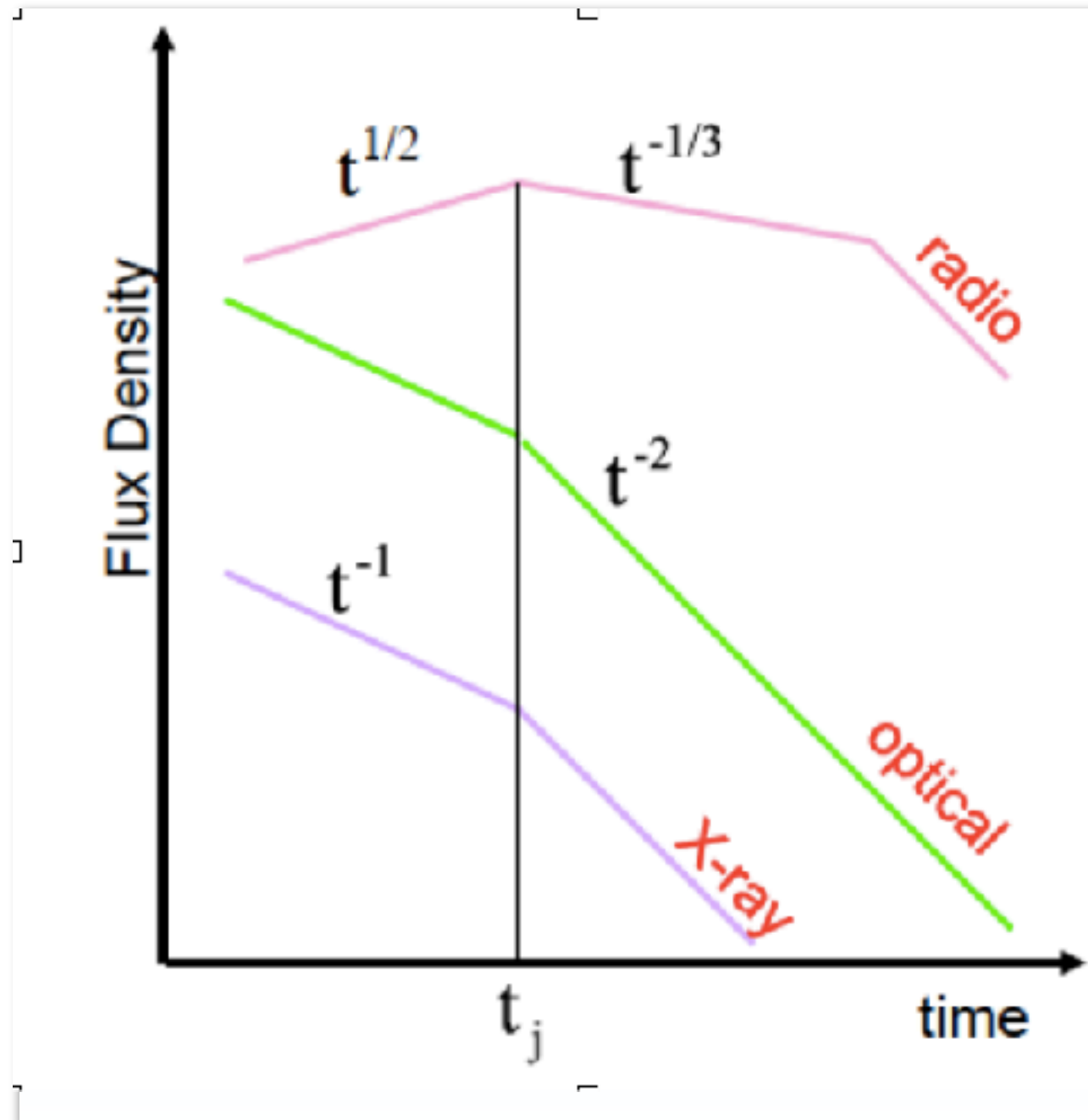
Synchrotron self absorption and circumburst density

PC et al. 2008



PC et al 2008

Collimation angle



$$\theta_j = 0.057 \left(\frac{t_j}{1 \text{ day}} \right)^{3/8} \left(\frac{1+z}{2} \right)^{-3/8} \left[\frac{E_{\text{iso}}(\gamma)}{10^{53} \text{ ergs}} \right]^{-1/8} \times \left(\frac{\eta_\gamma}{0.2} \right)^{1/8} \left(\frac{n}{0.1 \text{ cm}^{-3}} \right)^{1/8},$$

Energetics

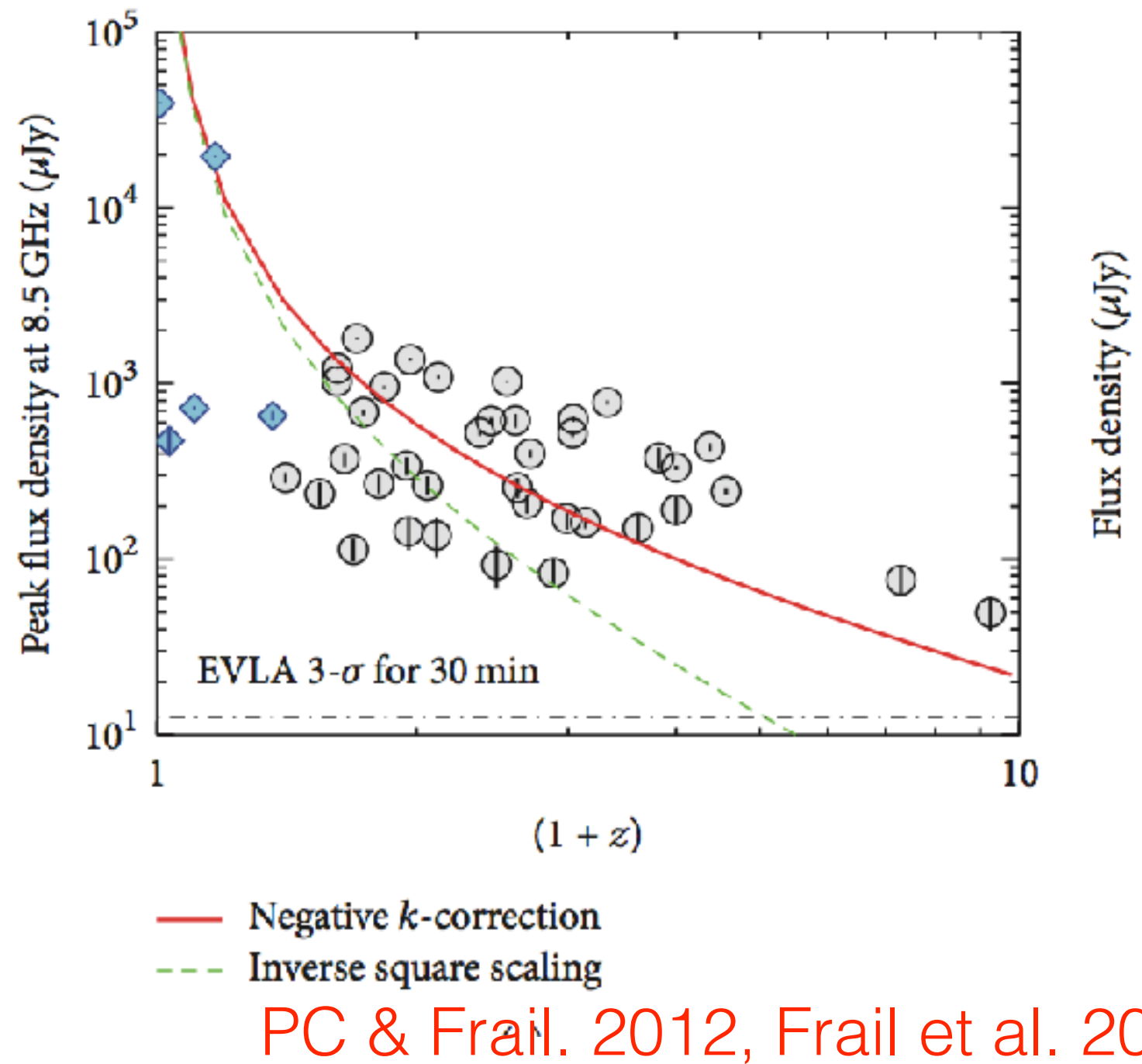
- A class of GRBs has total relativistic energy release at least an order of magnitude above the canonical value of 10^{51} erg (such as GRBs 050820A, 050904, 070125, 080319B, 090323, 090423, 090926A, [Chandra et al. 2008, 2010; Chandra & Frail 2011; Cenko et al. 2010, 2011](#)). The total energy budget of these hyper-energetic events poses a significant challenge for some progenitor models. However, due to limited bandpass of Swift-BAT captures only a small fraction of the total γ -ray energy, and can entirely miss the peak of the γ -ray spectrum. Fermi is sensitive to GRBs with very large isotropic energy releases (10^{54} erg), which are rare events (although important for testing the central engine models).
- An additional concern is the double-jet models for GRB 030329 ([Berger et al. 2003b; van der Horst et al. 2005](#)) and GRB 080319B ([Racusin et al. 2008](#))
- Late time radio afterglow observations, when the flow has become subrelativistic offer a unique insight into the energy problem. At late stages, the jet would have expanded sideways so much that it would essentially become quasi-spherical and independent of the jet geometry, giving handle of the accurate calorimetry of GRBs.
- Possible only for GRBs with bright radio afterglows. Higher sensitivity radio telescopes can observe the afterglow for a longer time and provide the accurate energy estimation.

Subrelativistic transition

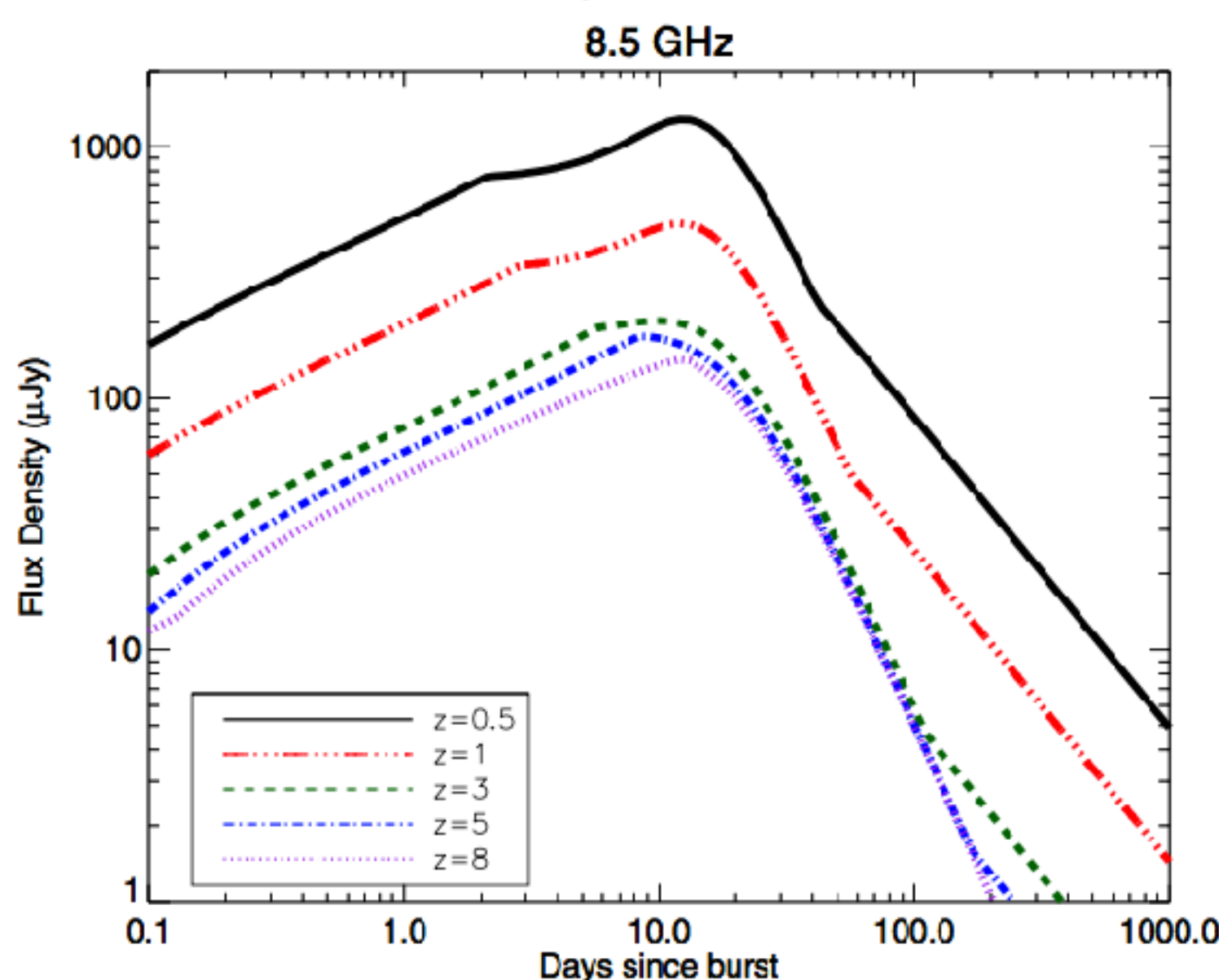
- GRB 970508 remained bright more than a year after the discovery, when the ejecta had reached sub-relativistic speeds making the energetics independent of geometry of the burst. This gave the most accurate estimate of the kinetic energy of the burst ($E_{KE} = 0.5 \times 10^{51}$ erg ([Frail et al. 2000b](#))).
- GRB 030329 has the longest lived radio afterglow. The inferred energetics from the sub-relativistic regime gives $E_{KE} = \text{few times } 10^{51}$ erg ([Frail et al. 2005](#))
- [Shivvers & Berger 2011](#) - sample of 24 GRBs with observations >100 days after the burst. Median energy 7×10^{51} erg, with a 90% confidence range of 1.1×10^{50} - 3.3×10^{53} erg.

Detectable at High redshift

- Negative-K correction:
Effects of cosmological redshift and time dilation counteracting the dimming due to source distance (Ciardi & Loeb 2000)



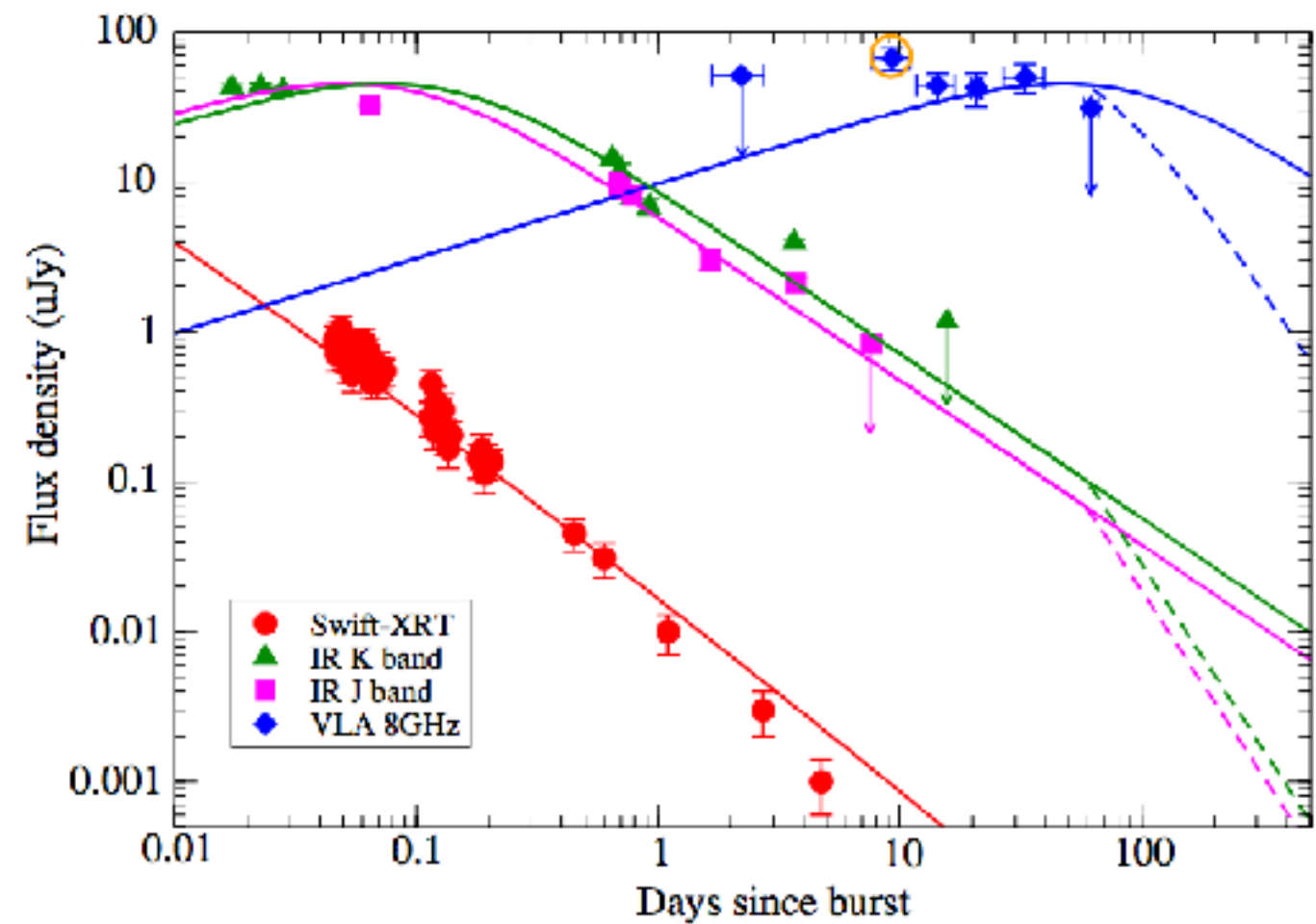
Weak redshift dependence



PC & Frail. 2011, 2012

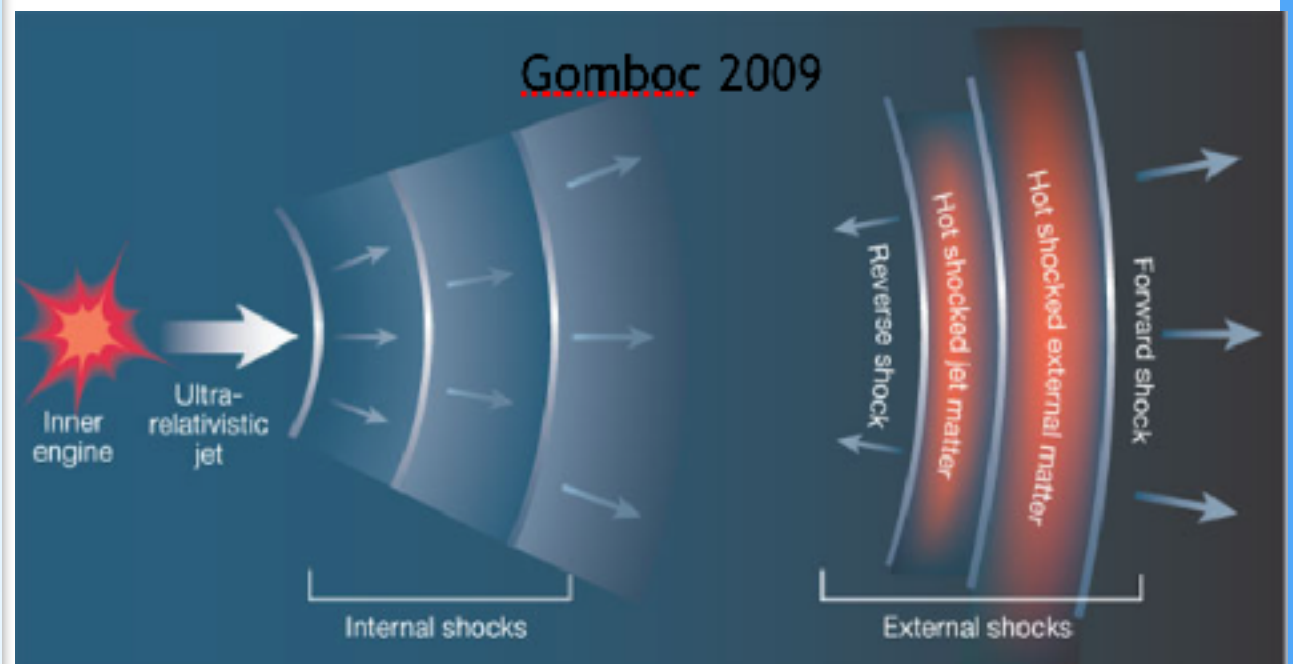
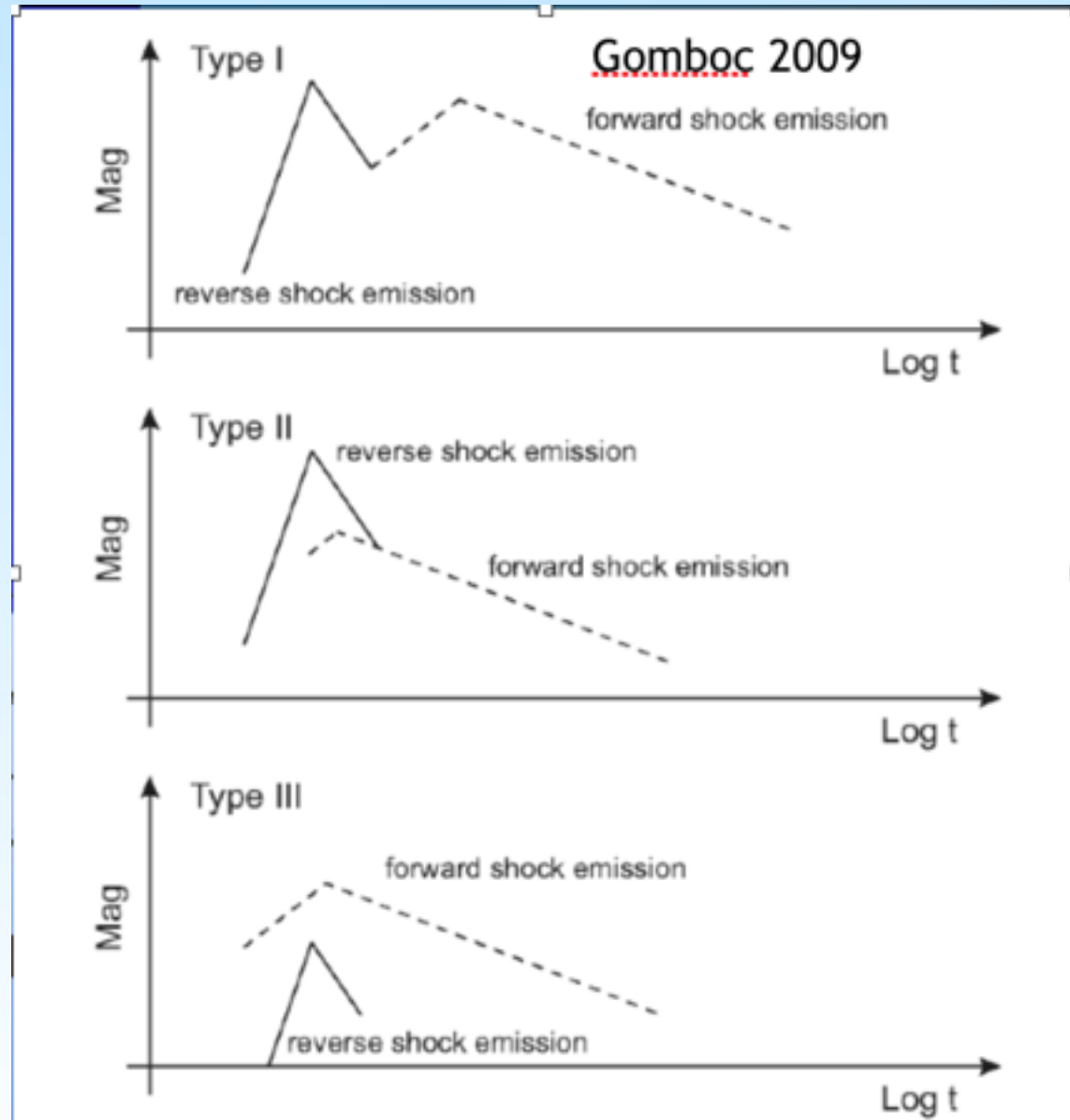
Highest spectroscopic redshift GRB 090423

- $z=8.3$
- Radio emission detected
- Indicated density ~ 1 cm^{-3}



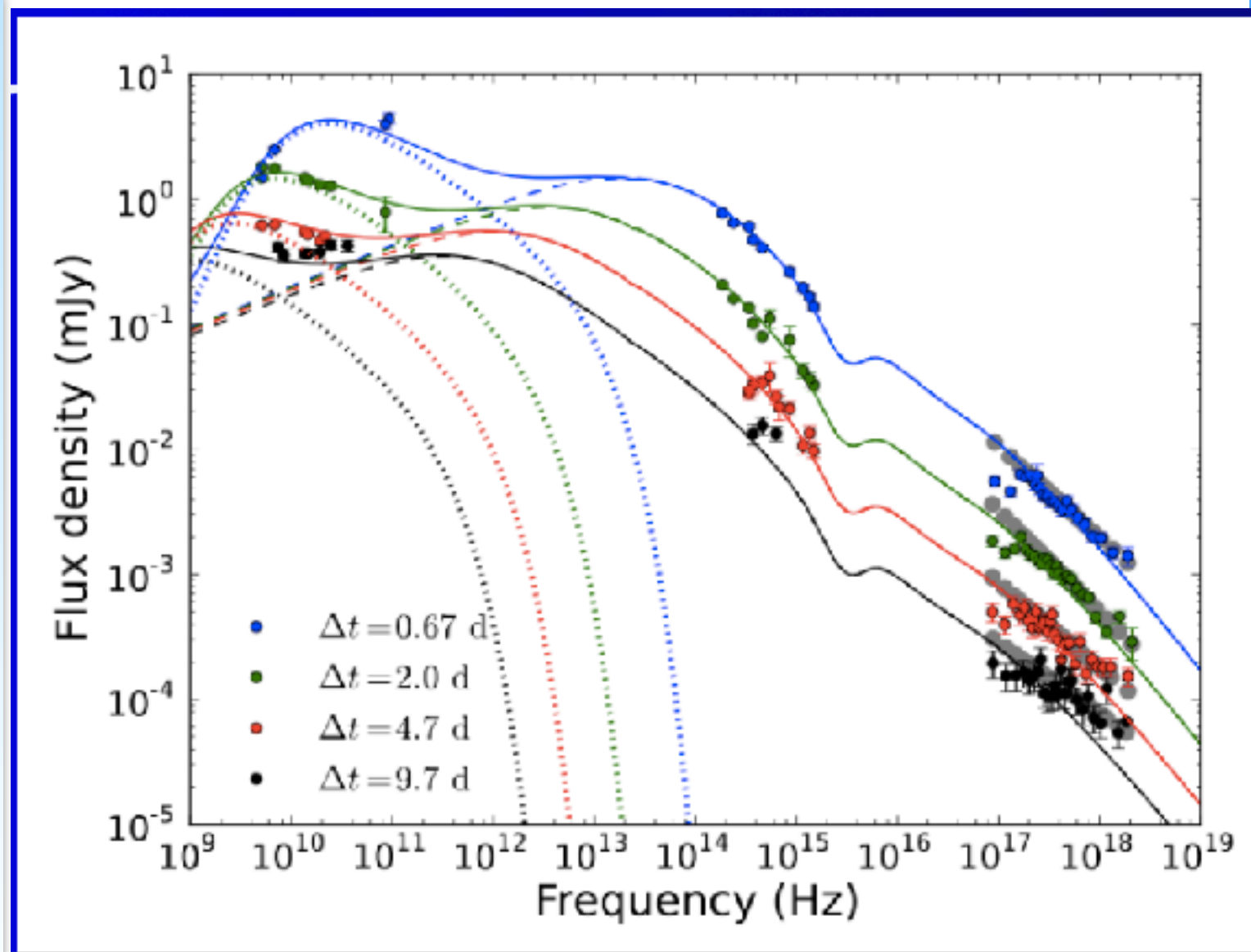
PC 2016, PC & Frail 2012

Reverse shock in GRBs



Reverse shock in GRB 130427A

- Emission modeled with two components - RS and FS
- RS peak evolution from high to low frequencies
- Low density environments seems favourable for radio RS, e.g. GRB 990123
(Granot & van Der Horst 2014)

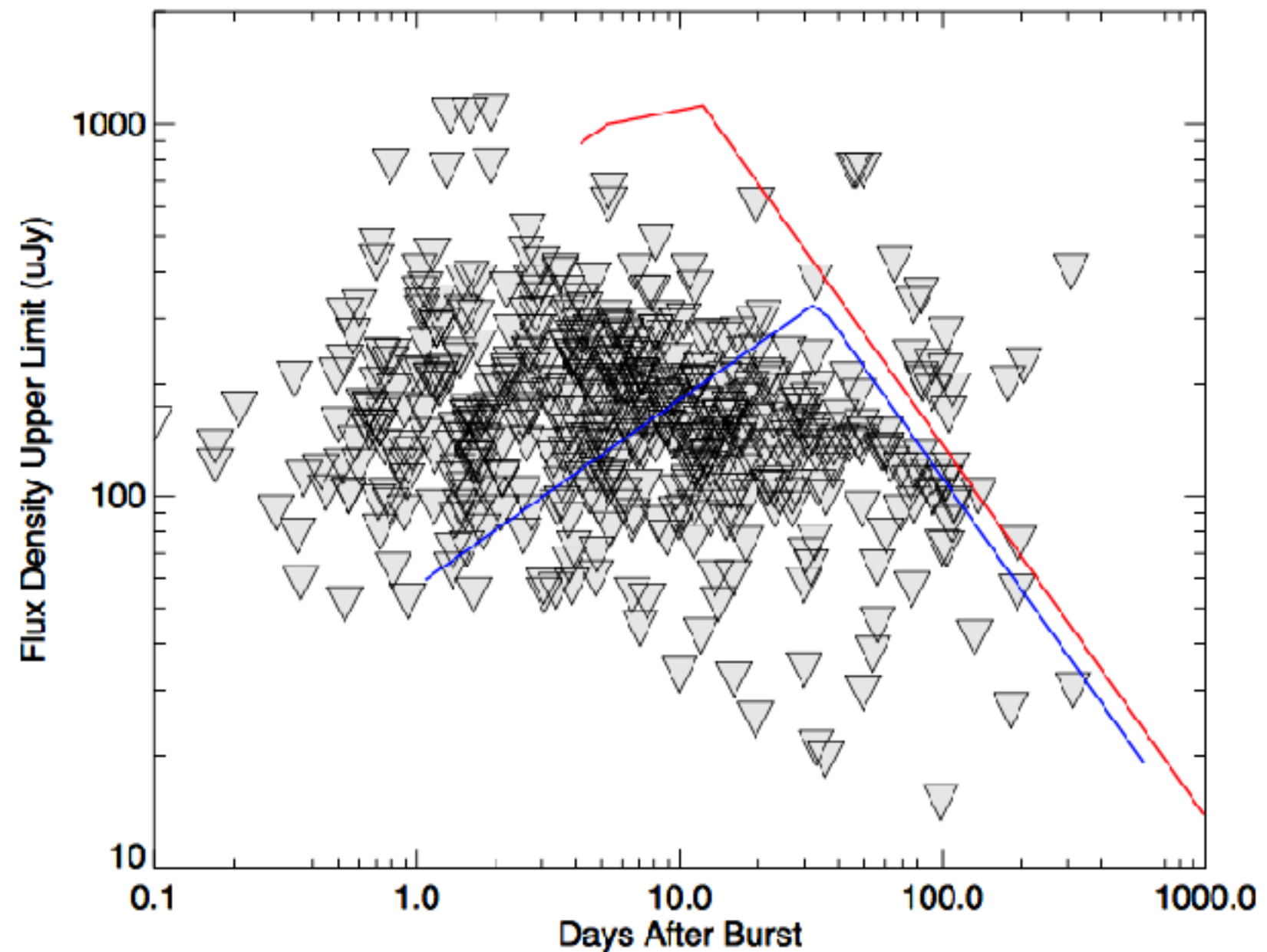


Laskar et al. 2013, Cenko et al. 2014

Sample of radio afterglows

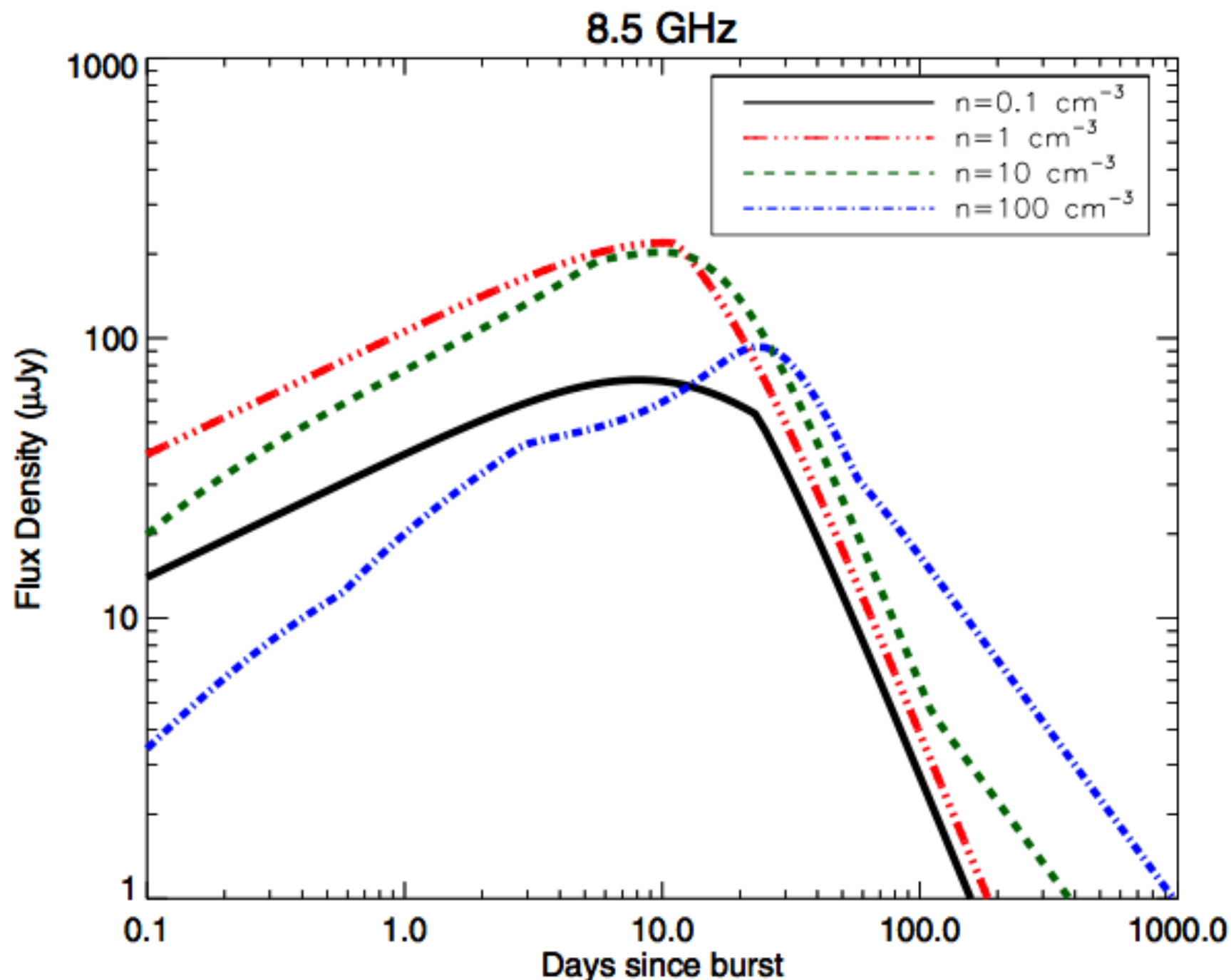
- While many of the early advances were made by studying individual GRBs and their afterglows, now much more can be learned from the study of large samples (Sakamoto et al. 2008, 2011).
- We compiled sample consisting of 304 GRBs observed with the radio telescopes between 1997 to 2011. This sample includes 35 Short-hard bursts (SHBs), 19 X-ray flashes (XRFs) and 25 GRBs with possible supernova associations (SN/GRBs) (PC & Frail 2011, 2012, PC 2016).
- A total of 95 out of 304 bursts were detected in radio bands, resulting in a detection rate of 31%. The radio detection statistics in pre-*Swift* and post-*Swift* samples essentially remained unchanged i.e. 42/123 (34%) in pre-*Swift* and 53/181 (29%) in post-*Swift*. In contrast, the X-ray detection rates increase from 41% to 93% after the launch of *Swift*. The optical detection rates also increased from 47% to 75% between pre-*Swift* and post-*Swift* bursts.

Non-detection - sensitivity limited



PC & Frail, 2012

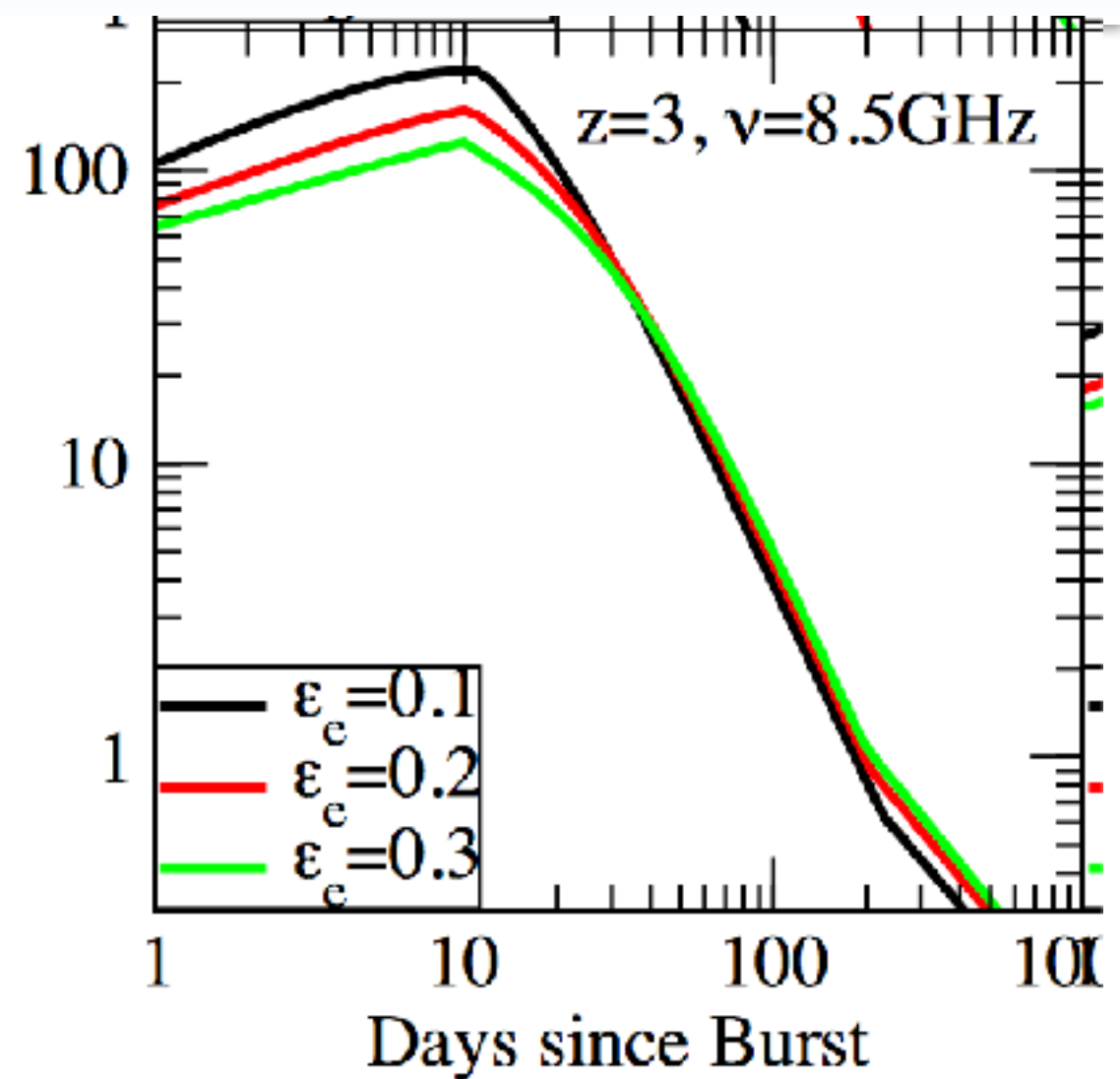
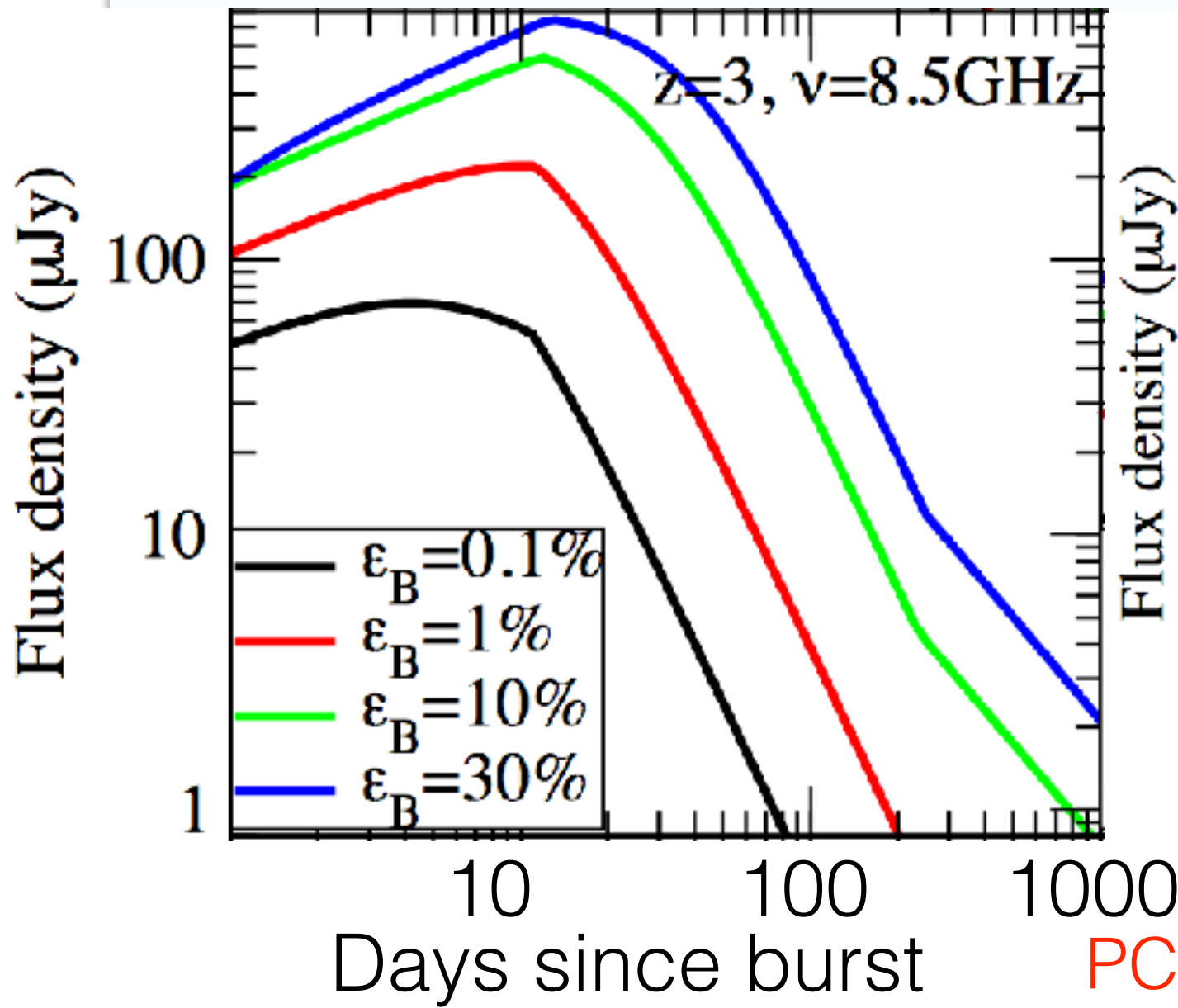
Radio afterglow and density



PC & Frail 2011, 2012

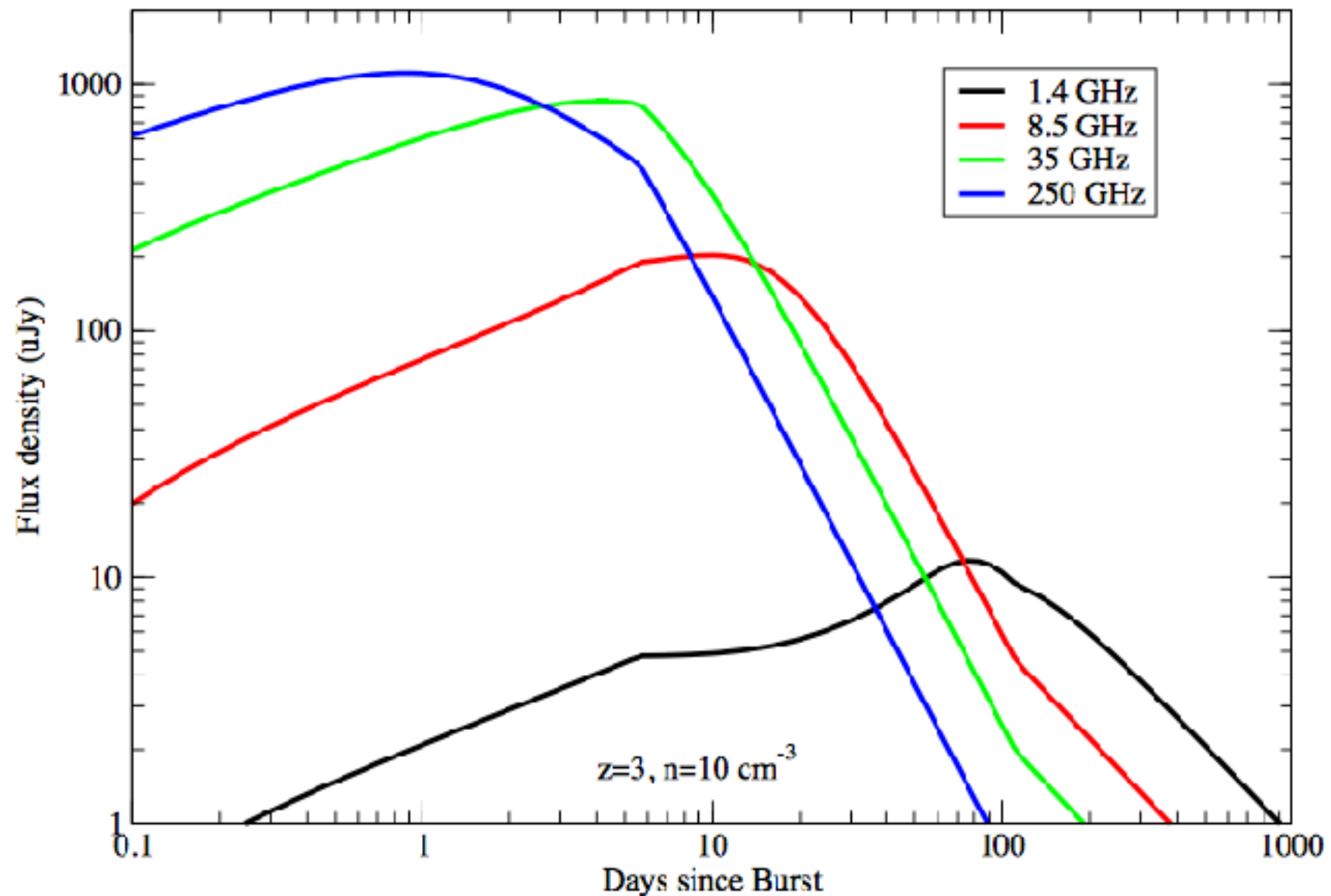
Radio afterglow on microscopic parameters

If less amount of energy goes in magnetic field and more energy goes to electrons, radio emission will not be strong enough to be detectable.



PC & Frail 2011, 2012

Optimum frequency

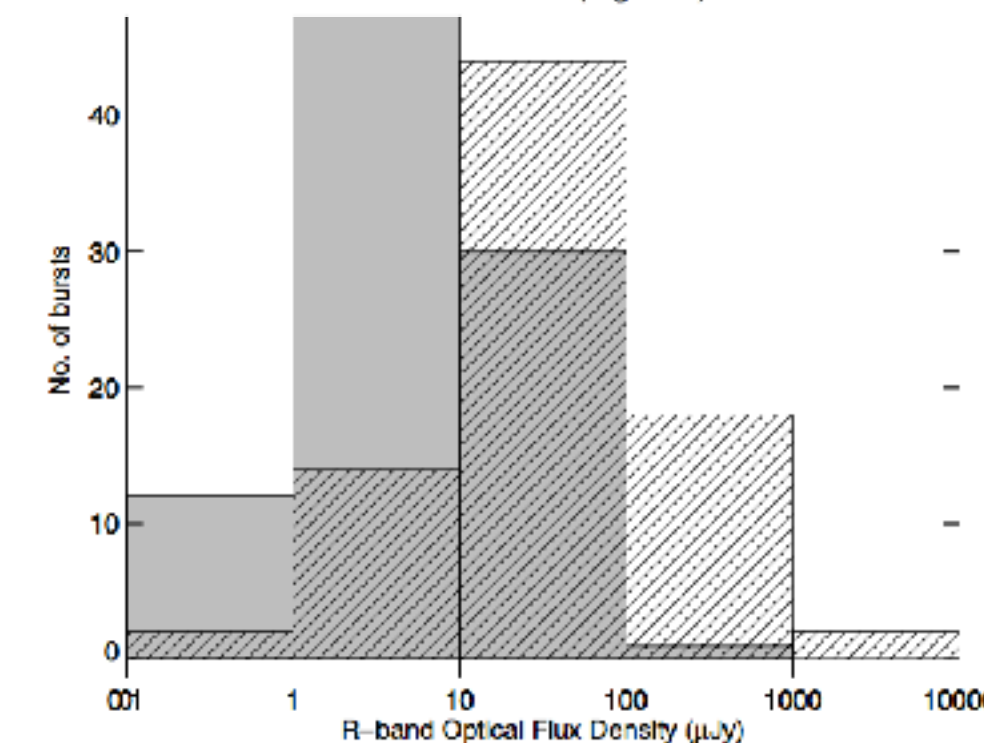
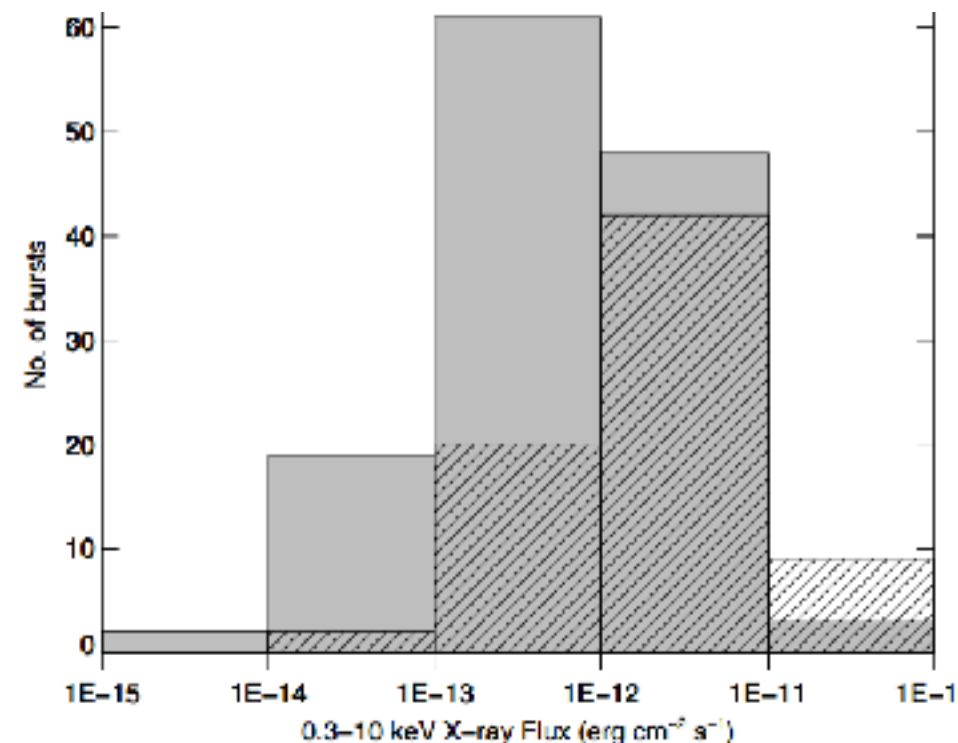
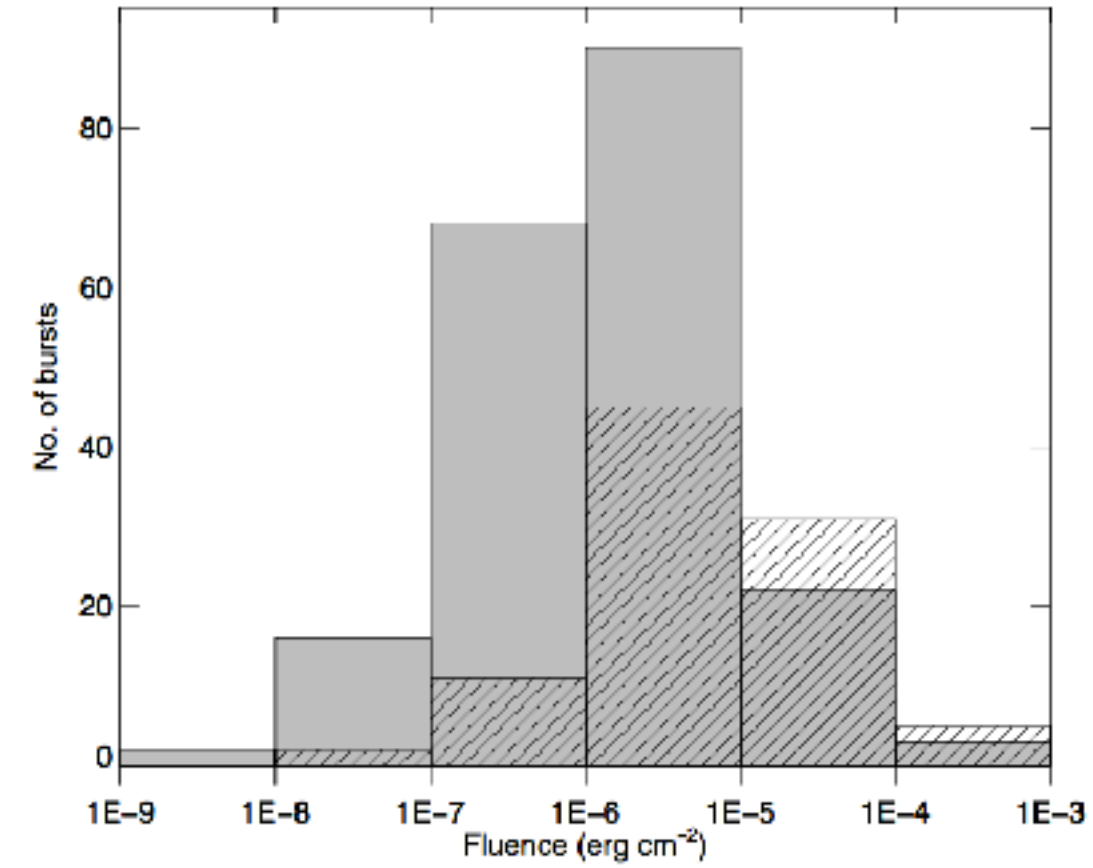
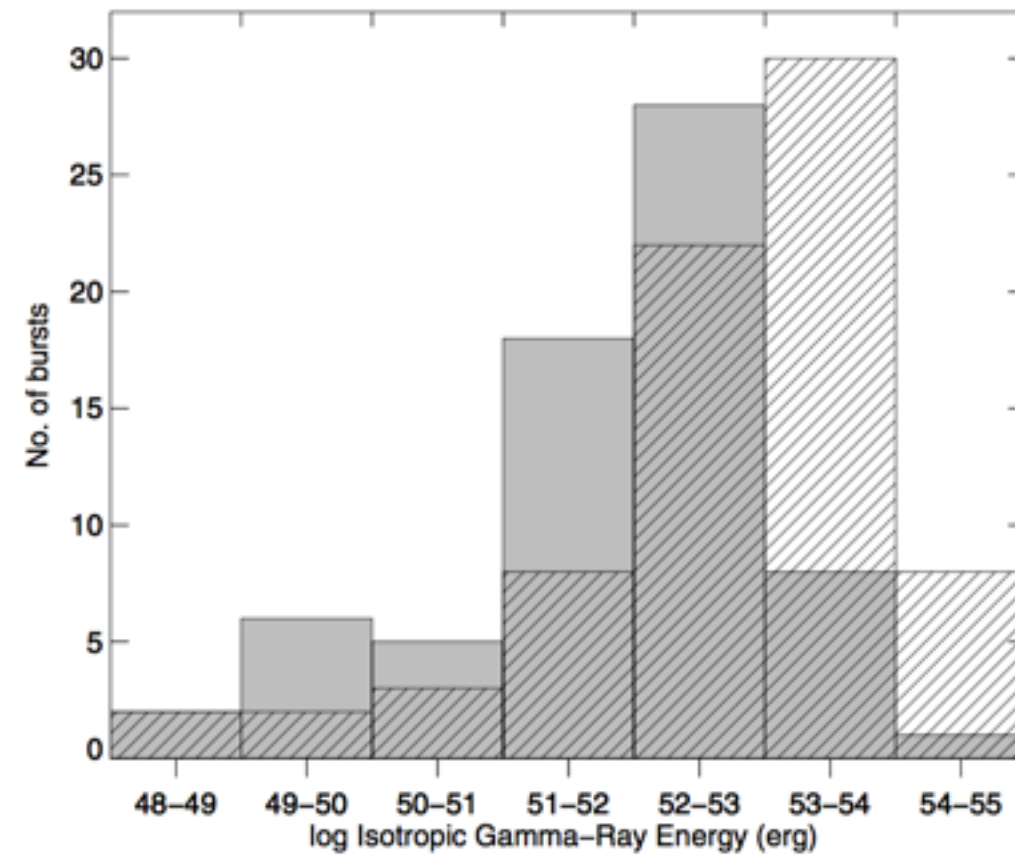


PC & Frail 2011, 2012

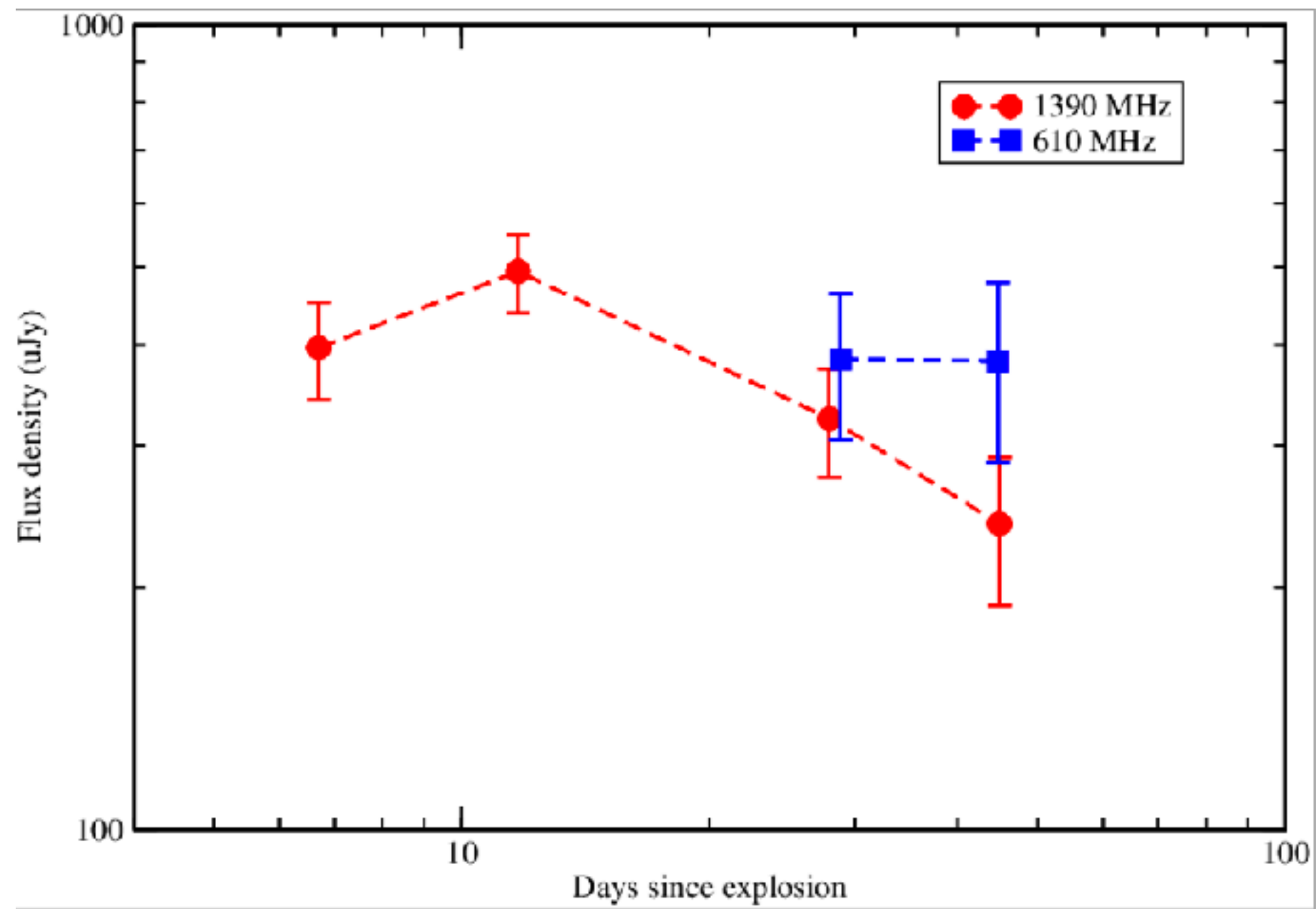
Intrinsic differences

- Hancock et al. 2013 - intrinsically different population of GRBs. No more than 60-70% GRBs truly radio bright.
- If more energy goes into isotropic emission, less energy available as ejecta kinetic energy.
- Black hole engine GRBs - no radio emission
- Magnetar engine GRBs - detectable radio emission

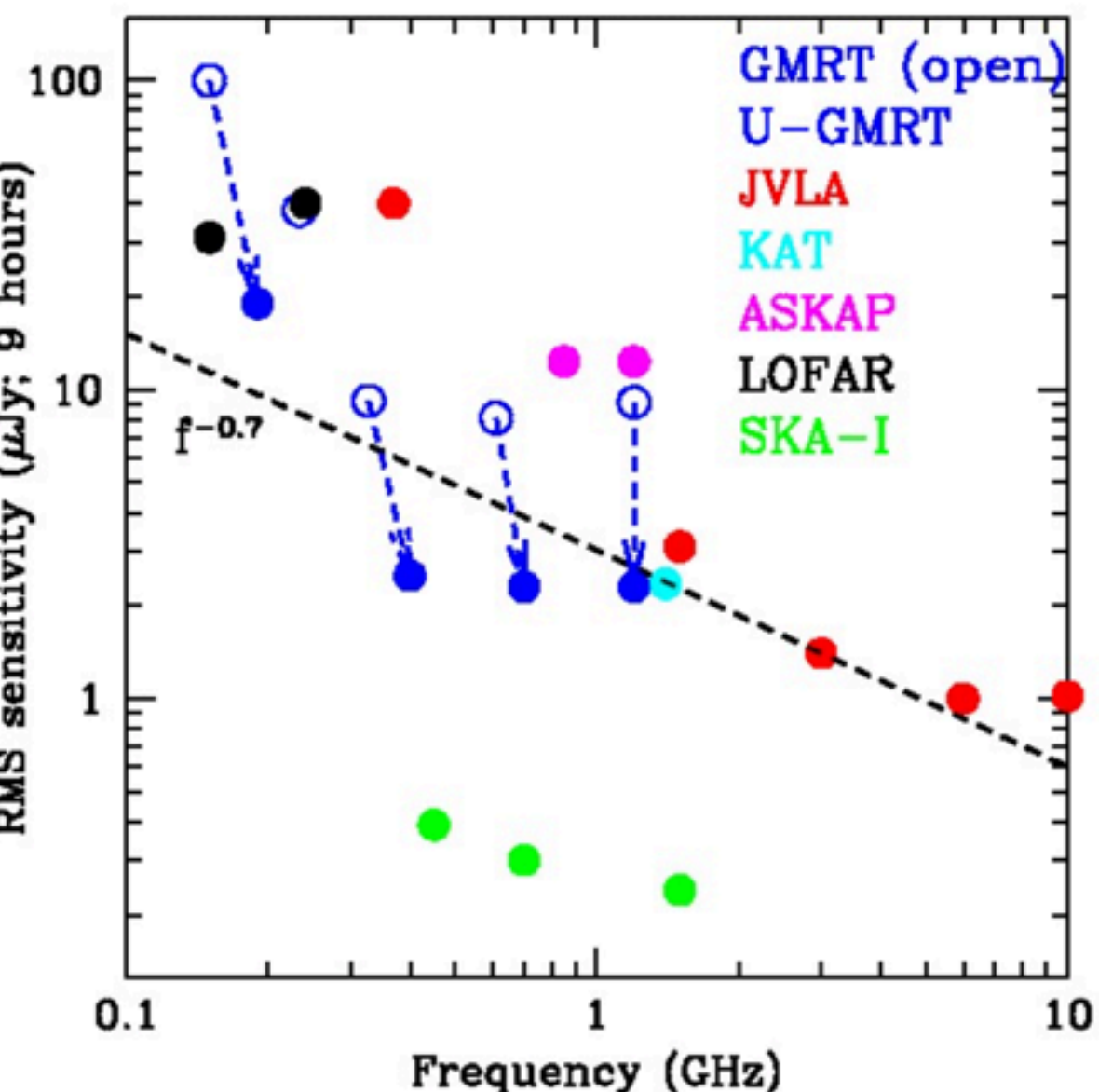
Dependence of radio afterglow detectability



Nature of circumburst density



In preparation



Giant Metrewave Radio Telescope

